A Diarylethene with Two Nitronyl Nitroxides: Photoswitching of Intramolecular Magnetic Interaction

Kenji Matsuda* and Masahiro Irie*

Contribution from Department of Chemistry and Biochemistry, Graduate School of Engineering, Kyushu University, and CREST, Japan Science and Technology Corporation, 6-10-1 Hakozaki, Higashi-ku, Fukuoka, 812-8581, Japan

Received February 18, 2000. Revised Manuscript Received May 1, 2000

Abstract: A diarylethene having two nitronyl nitroxides, 1,2-bis[6-(1-oxyl-3-oxide-4,4,5,5-tetramethylimidazolin-2-yl)-2-methyl-1-benzothiophen-3-yl]hexafluorocyclopentene (**2a**), was synthesized in an attempt to control the intramolecular magnetic interaction by photoirradiation. The photochemical conversions from open-ring isomer **2a** to closed-ring isomer **2b** and from **2b** to **2a** were both almost 100%. Magnetic measurement revealed the antiferromagnetic interaction between two nitronyl nitroxides remarkably increased from $2J/k_B = -2.2$ K to $2J/k_B = -11.6$ K when the diarylethene spin coupler was switched from the open-ring isomer **2a** to the closed-ring isomer **2b**. ESR measurements were also carried out for both **2a** and **2b** in benzene solutions at room temperature and in MTHF solid solutions at cryogenic temperature. Both ESR and magnetic measurement indicated that the intramolecular interaction was switched by the photochromic spin coupler.

Introduction

Photochromism is defined as light-induced reversible transformation of chemical species between two isomers having different absorption spectra.[1] The two isomers differ from each other not only in the absorption spectra but also in various physical and chemical properties, such as geometrical structure, refractive index, dielectric constant, and oxidation/reduction potentials. These property changes have been utilized to control functions of photoresponsive molecules and polymers, such as host−guest interactions,[2] various physical properties of polymers,[3] alignment of liquid crystals,[4] nonlinear optical properties,[5] and electronic conduction.[6]

Molecular magnetism[7] can also be photocontrolled by incorporating a photochromic moiety into the system. Although so far, intermolecular magnetic interaction has been photochemically controlled by electron transfer,[8] by spin crossover of the metal ion,[9] or by intercalation of a photochromic compound with metallic compounds,[10] photocontrol of intramolecular magnetic interaction in a molecule has not yet been achieved.[11]

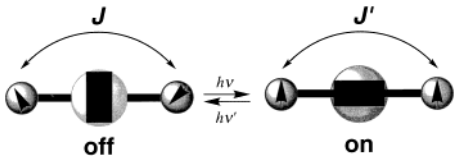

Figure 1. Photoswitching of magnetic interaction.

When two open-shell moieties were placed at the edges of a π-conjugative molecule, two electronic spins interact magnetically through the π-conjugative framework by exchange interaction *J*. The sign of the exchange interaction depends on the topology of the π-system. If we can change the strength of the coupler by external stimulation, we can control the magnetism of the system. In this paper, we report on the photoswitching of the intramolecular magnetism by incorporating two radical moieties into a photochromic diarylethene spin coupler (Figure 1).

Results and Discussion

Molecular Design and Synthesis. Diarylethenes undergo a hexatriene−cyclohexadiene-type photochromic reaction (Scheme 1). They exhibit excellent photochromic performance: thermal stability of both isomers even at 100 °C, high fatigue resistance (>10^4 coloration/decoloration cycles), and very rapid response (∼1 ps). The diarylethene family is one of the most promising photochromic materials for applications to optoelectronics.

(1) (a) Brown, G. H. *Photochromism*; Wiley-Interscience: New York, 1971. (b) Dürr, H.; Bouas-Laurent, H. *Photochromism*: *Molecules and Systems*; Elsevier: Amsterdam, 1990. (c) Irie, M.; Uchida, K. *Bull. Chem. Soc. Jpn.* **1998**, *71*, 985.

(2) (a) Desvergne, J.-P.; Bouas-Laurent, H. *J. Chem. Soc., Chem. Commun.* **1978**, 403. (b) Shinkai, S. *Pure Appl. Chem.* **1987**, *59*, 425. (c) Blank, M.; Soo, L. M.; Wasserman, N. H.; Erlanger, B. F. *Science* **1981**, *214*, 70. (d) Irie, M.; Kato, M.; *J. Am. Chem. Soc.* **1985**, *107*, 1024. (e) Takeshita, M.; Irie, M. *J. Org. Chem.* **1998**, *63*, 6643.

(3) (a) Irie, M.; Hirano, Y.; Hashimoto, S.; Hayashi, K. *Macromolecules* **1981**, *14*, 262. (b) Irie, M. *Adv. Polym. Sci.* **1990**, *94*, 27. (c) Irie, M. *Adv. Polym. Sci.* **1993**, *110*, 49.

(4) (a) Ichimura, K.; Suzuki, Y.; Seki, T.; Hosoki, A.; Aoki, K. *Langmuir* **1988**, *4*, 1214. (b) Ikeda, T.; Sasaki, T.; Ichimura, K. *Nature* **1993**, *361*, 428.

(5) Atassi, Y.; Delaire, J. A.; Nakatani, K. *J. Phys. Chem.* **1995**, *99*, 16320.

(6) (a) Gilat, S. L.; Kawai, S. H.; Lehn, J.-M. *J. Chem. Soc., Chem. Commun.* **1993**, 1439. (b) Gilat, S. L.; Kawai, S. H.; Lehn, J.-M. *Chem. Eur. J.* **1995**, *1*, 275. (c) Kawai, T.; Kunitake, T.; Irie, M. *Chem. Lett.* **1999**, 905.

(7) Kahn, O. *Molecular Magnetism*; VCH: New York, 1993.

(8) (a) Sato, O.; Iyoda, T.; Fujishima, A.; Hashimoto, K. *Science* **1996**, *272*, 704. (b) Gu, Z.-Z.; Sato, O.; Iyoda, T.; Hashimoto, K.; Fujishima, A. *J. Phys. Chem.* **1996**, *100*, 18289.

(9) (a) Boillot, M.-L.; Roux, C.; Audière, J.-P.; Dausse, A.; Zarembowitch, J. *Inorg. Chem.* **1996**, *35*, 3975. (b) Boillot, M.-L.; Chantraine, S.; Zarembowitch, J.; Lallemand, J.-Y.; Prunet, J. *New J. Chem.* **1999**, 179.

(10) Fujita, W.; Awaga, K. *J. Am. Chem. Soc.* **1997**, *119*, 4563.

(11) (a) Hamachi, K.; Matsuda, K.; Itoh, T.; Iwamura, H. *Bull. Chem. Soc. Jpn.* **1998**, *71*, 2937. (b) Matsuda, K.; Irie, M. *Chem. Lett.* **2000**, 16, a preliminary communication of this paper.

10.1021/ja000605v CCC: $19.00
Published on Web 07/11/2000

Scheme 1. Photochromic Diarylethenes

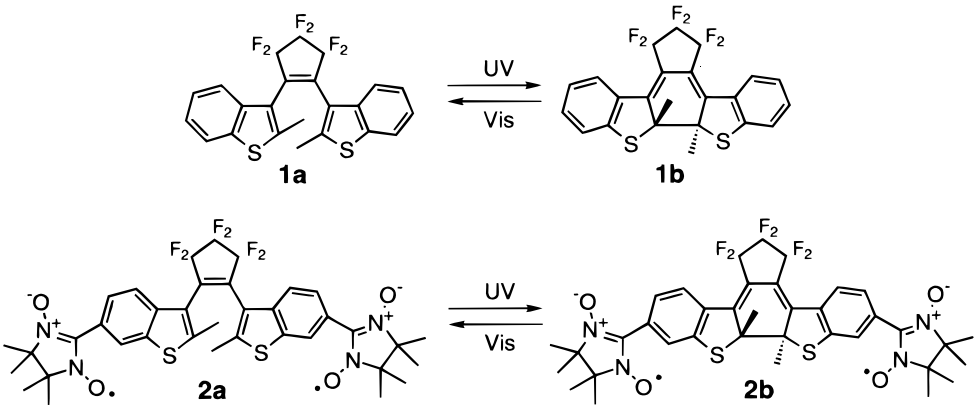

There is a characteristic feature in the electronic structural changes of diarylethenes. Scheme 2 shows the open-ring isomer **3a** and closed-ring isomer **3b** of the radical-substituted diarylethenes. While there is no resonant closed-shell structure for **3a**, there exists **3b′** as the resonant quinoid-type closed-shell structure for **3b**. **3a** is classified as a non-Kekulé diradical, and **3b** is classified as a normal Kekulé molecule. In other words, **3a** has two unpaired electrons and **3b** has no unpaired electrons. To know the exchange interaction between two spins of **3a**, the shape of two singly occupied molecular orbitals (SOMOs) was calculated by the MNDO UHF method (Figure 2a).[12] The two SOMOs are separated in the molecule and there is no overlap. This configuration is a typical disjoint diradical,[13] such as tetramethyleneethane, in which intramolecular radical−radical interaction is weak. In the open-ring isomer, bond alternation is disconnected at the 3-position of the thiophene rings. This is the origin of the disjointed nature of the electronic configuration of **3a**.

Scheme 2[a]

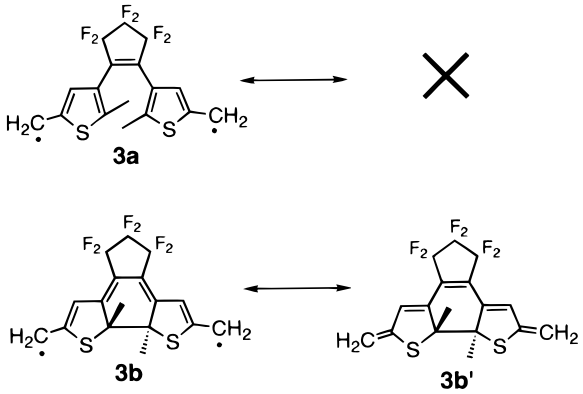

[a] Reagents and conditions: (a) dichloromethyl methyl ether, $AlCl_3$, nitrobenzene, 82%. (b) 2,3-dimethyl-2,3-bis(hydroxyamino)butane sulfate, methanol and then $NaIO_4$, CH_2Cl_2, 16%.

The MNDO RHF calculation was also carried out for the closed-ring isomer **3b′**. The shape of the HOMO is shown in Figure 2b. The normal bond alternation is clearly shown, indicating this molecule is a normal Kelulé molecule.

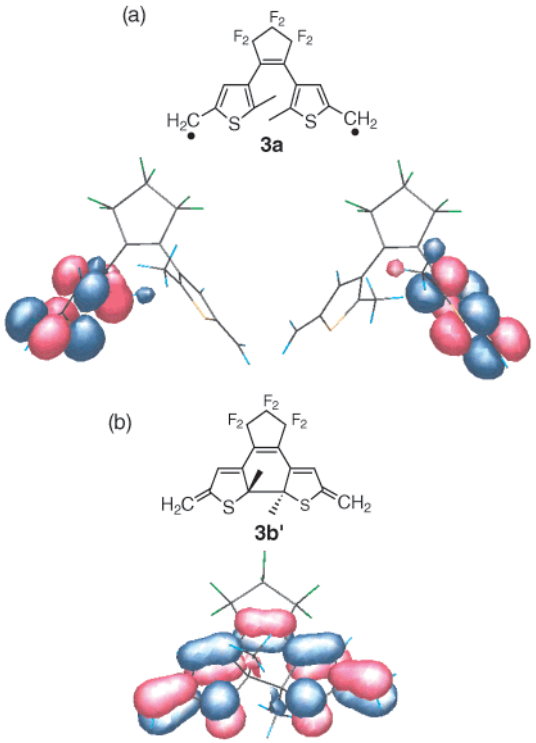

Figure 2. (a) Shape of the two SOMOs of **3a** calculated at the MNDO UHF level. (b) Shape of HOMOs of **3b′** calculated at the MNDO RHF level.

The electronic structural changes of radical-substituted diarylethenes along with the photoisomerization is the change from a disjointed non-Kekulé structure to a closed-shell Kekulé structure. It is inferred from the above consideration that the interaction between spins in the open-ring isomer of diarylethene is weak, while significant antiferromagnetic interaction takes place in the closed-ring isomer. In other words, the open-ring isomer is the "off" state and the closed-ring isomer is the "on" state.

We chose 1,2-bis(2-methyl-1-benzothiophen-3-yl)perfluorocyclopentene (**1a**) as a photochromic spin coupler (Scheme 1). **1a** is one of the most fatigue-resistant diarylethenes.[14] Nitronyl nitroxide was chosen for the spin source, because this radical is π-conjugative. Thus, we designed molecule **2a**, which is one of the concrete models of **3a** (Scheme 1).

(12) Calculation and visualization of molecular orbital was performed on a MOPAC 97 program in WinMOPAC ver. 2 of Fujitsu Co. at Chiba, Japan.

(13) The term "disjoint" means that two SOMO of diradical are placed in such a configuration that the two spins cannot have exchange interaction. See: (a) Borden, W. T.; Davidson, E. R. *J. Am. Chem. Soc.* **1977**, *99*, 4587. (b) Matsuda, K.; Iwamura, H. *J. Am. Chem. Soc.* **1997**, *119*, 7412.

(14) (a) Uchida, K.; Nakayama, Y.; Irie, M. *Bull. Chem. Soc. Jpn.* **1990**, *63*, 1311. (b) Hanazawa, M.; Sumiya, R.; Horikawa, Y.; Irie, M. *J. Chem. Soc., Chem. Commun.* **1992**, 206.

Scheme 3

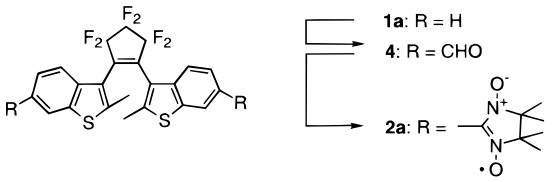

The synthesis was performed according to Scheme 3. **1a** was formylated by dichloromethyl methyl ether to give diformyl compound **4**. Then, **4** was treated with 2,3-bis(hydroxyamino)-2,3-dimethylbutane sulfate followed by sodium periodate. **2a** was obtained and purified by column chromatography and gel permeation chromatography (GPC). Recrystallization from hexane−CH_2Cl_2 gave a dark blue plate crystal of **2a**. The structure of **2a** was confirmed by ESR and mass spectroscopy and finally by X-ray crystallography (vide infra).

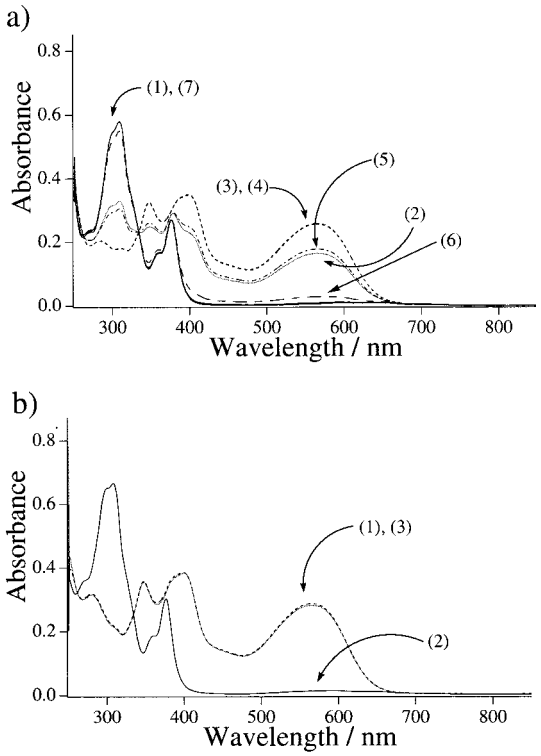

Figure 3. UV−visible absorption spectra measured at different stages of photochromic reaction: (a) starting from open-ring isomer **2a** (1.7×10^{-5} M AcOEt solution). (1) Initial and (2) after irradiation with 313-nm light for 1, (3) 5, and (4) 10 min (5) after irradiation with 578-nm light for 5, (6) 30, and (7) 60 min. (b) Starting from closed-ring isomer **2b** (1.9×10^{-5} M AcOEt solution). (1) Initial and (2) after irradiation with 578-nm light for 60 min (3) after irradiation with 313-nm light for 5 min.

Photochromic Reaction. Figure 3 shows the photochromic interconversion between **2a** and **2b**. The ethyl acetate solution of **2a** (1.7×10^{-5} M) was irradiated with 313-nm light. Upon irradiation, the intense absorption at 565 nm grew and after 5 min it reached the photostationary state. A clear isosbestic point was observed at 334 nm. Then the sample was irradiated with 578-nm light for 60 min. The spectrum converted back to the original one with retention of the isosbestic point at 334 nm. Although the radical moiety has absorption around 550−700 nm, it did not prohibit the photochromic reaction.

Similar photochromic behavior was also observed starting from closed-ring isomer **2b.** Upon irradiation with 578-nm light, the absorbance at 565 nm almost disappeared. The remaining absorption is due to the radicals. After that the solution was irradiated with 313-nm light, the absorption returned perfectly to the initial closed-ring isomer **2b**, suggesting the conversion from **2a** to **2b** is almost 100%. For practical usage of photochromic materials, high conversion is one of the important characteristics.

The color of the solution was interconverted from blue in **2a** to red-purple in **2b**. The effect of the radical moiety, which possesses blue color, will be discussed in the next section.

Table 1. Quantum Yields and Conversions of Photochromic Reactions of **1a**, **1b**, **2a**, and **2b** in Ethyl Acetate

diarylethene	Φ	conversion/%
1a → **1b**	0.31[a]	43[a]
1b → **1a**	0.28[b]	100[b]
2a → **2b**	0.040[a]	100[a]
2b → **2a**	0.0010[b]	100[b]

[a] Measured at 313 nm. [b] Measured at 517 nm.

Effect of Radical on Quantum Yield. It is indispensable to investigate the quantum yields of photochromic reactions for the design of high-sensitive and high-conversion photochromic units. The quantum yields of both cyclization and cycloreversion reactions of **1a** and **2a** and conversions in the photostationary state were measured in ethyl acetate. The results are summarized in Table 1.

The quantum yield of cyclization reaction of **2a** was $\sim 1/8$ of the value of **1a**. The cycloreversion reaction was also strongly suppressed. This is due to the contribution of the resonant quinoid structure **2b′** (Scheme 4). The low cycloreversion quantum yield resulted in the high conversion from open-ring isomer **2a** to closed-ring isomer **2b**. Lehn et al. reported that the closed-ring isomer of bis-phenolic diarylethenes could be electrochemically oxidized to the quinoid form and the photochromism was locked.[6b] In our case, the contribution of the quinoid structure was not so large. Therefore, a reversible photochromic reaction took place.

Switching of Molecular Structure. Both isomers **2a** and **2b** could be isolated as crystals. The crystal structure was determined by X-ray crystallographic analysis. The crystallographic data are summarized in Table 2. Figure 4 shows ORTEP drawings of the open-ring isomer **2a** and the closed-ring isomer **2b**. **2a** had a twisted structure. The dihedral angle between benzothiophene ring and perfluorocyclopentene ring was 86.1°, suggesting disconnection of π-conjugation between the benzothiophene ring and the ethene moiety. The nearest intermo-

Scheme 4

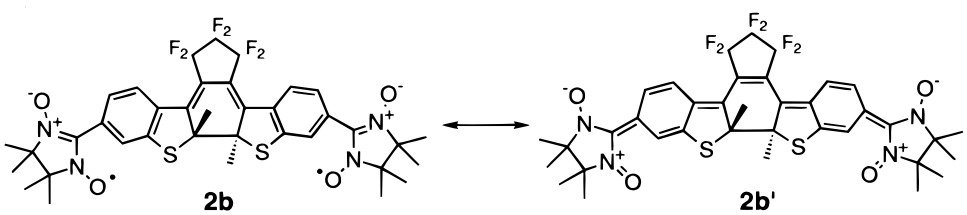

Table 2. Crystallographic Parameters for **2a** and **2b**

	2a	**2b**
formula	$C_{37}H_{36}F_6N_4O_4S_2$	$C_{38}H_{38}Cl_2F_6N_4O_4S_2$
formula weight	778.82	863.74
crystal color	dark blue	black
crystal system	triclinic	monoclinic
space group	$P\bar{1}$	$P2_1/c$
a/Å	11.537(5)	12.2767(18)
b/Å	12.256(5)	23.850(4)
c/Å	14.568(6)	26.549(4)
α/deg	85.023(8)	
β/deg	72.660(8)	90.513(3)
γ/deg	71.030(7)	
V/Å^3	1859.3(14)	7773(2)
Z	2	8
data/restraints/parameters	8638/0/476	8143/0/1001
R_1	0.0859	0.1153
wR_2	0.2112	0.2893

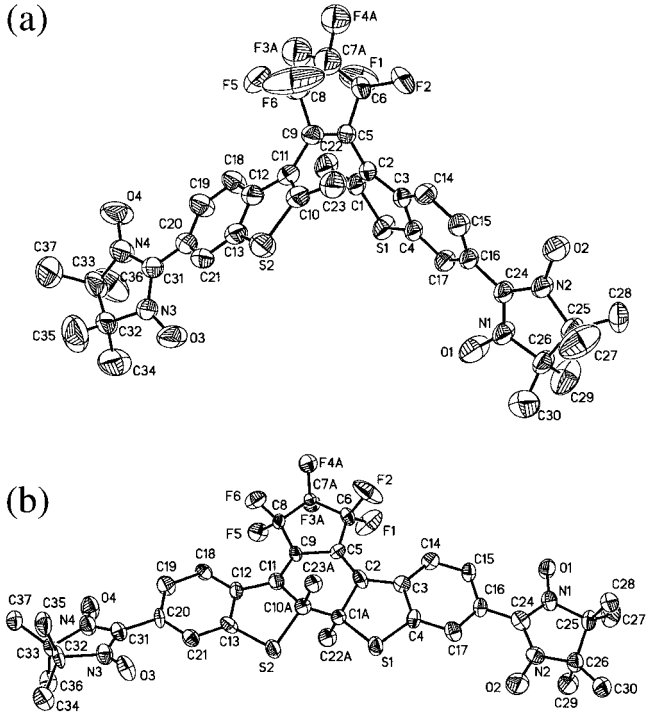

Figure 4. ORTEP drawings of (a) **2a** and (b) **2b** with thermal ellipsoids (50% probability). The hydrogen atoms are omitted for clarity. For **2b**, the solvent molecule is omitted. For **2b**, one of the two identical molecules is shown.

lecular contact between oxygen atoms of nitroxides was 4.38 Å, suggesting intermolecular magnetic interaction is negligible. The dihedral angle between the imidazoline ring and benzothiophene ring was 30.0°, suggesting π-conjugation between them. The distance between reactive carbons was 4.72 Å, which is too long to photochemically react in the crystalline phase. Photochromism in the crystalline phase was not observed.[15]

There were two crystallographically independent molecules in the crystal of **2b**. The two molecules were almost identical except for the dihedral angle between nitronyl nitroxide and the benzothiophene ring. The crystal contained one dichloromethane per one **2b** molecule. The dihedral angle between the benzothiophene ring and perfluorocyclopentene ring was 2.6°. π-Electrons were delocalized throughout the molecule. The bond length could be interpreted by the structure of **2b** not **2b′**,

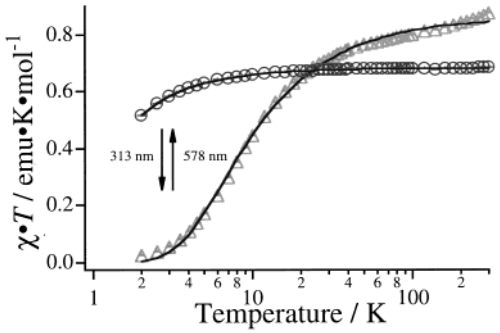

Figure 5. $\chi T-T$ plot for (○) **2a** and (△) **2b** measured at 5000 G. Solid line represents the theoretical curve (see text).

Table 3. Fitting Parameters of the Magnetic Data for Diradical **2a** and **2b**

diradical	$2J/k_B$K	θ/K	f
2a	-2.2 ± 0.04	0.24 ± 0.01	0.91
2b	-11.6 ± 0.4	-2.4 ± 0.3	1.14

indicating that the contribution of the quinoid structure is small. The intermolecular contact of nitronyl nitroxide was 3.62 Å, which is rather short to ignore the intermolecular interaction. The effect of intermolecular interaction was taken into account in the analysis of magnetic interactions shown below.

Switching of Magnetism. The magnetic susceptibilities of **2a** and **2b** were measured on a SQUID susceptometer in microcrystalline form. $\chi T-T$ plots are shown in Figure 5. The data were analyzed in terms of a modified singlet−triplet two-spin model (the Bleaney−Bowers type) in which two spins ($S = {}^1/_2$) couple antiferromagnetically within a biradical molecule by exchange interaction J (eq 1).[16] θ indicates a Weiss constant

$$\chi_{mol}T = f\frac{2Ng^2\mu_B{}^2T}{k_B(T-\theta)}\frac{1}{3+\exp(-2J/k_BT)} \qquad (1)$$

employed to describe the additional intermolecular interaction by a mean field theory. Correction factor f was introduced for correction of the experimental error. The best-fit parameters by means of a least-squares method were $2J/k_B = -2.2 \pm 0.04$ K, $\theta = 0.24 \pm 0.01$ K, and $f = 0.91$ for **2a** and $2J/k_B = -11.6 \pm 0.4$ K, $\theta = -2.4 \pm 0.3$ K, and $f = 1.14$ for **2b** (Table 3).[17] Although the interaction ($2J/k_B = -2.2$ K) between two spins in the open-ring isomer **2a** was small, spins of **2b** have a remarkable antiferromagnetic interaction ($2J/k_B = -11.6$ K).

We measured the magnetic susceptibility of **2b** (3% w/w) doped in poly(*n*-butyl methacrylate) to eliminate the contribution of the intermolecular interaction in the closed-ring form crystal. The measured intramolecular antiferromagnetic interaction in the polymer dispersed system ($2J/k_B = -12.5 \pm 0.5$ K) was similar to that observed in the crystal. This clearly indicates that the increase in $|2J/k_B|$ is not due to intermolecular interaction but due to the intramolecular interaction.

The open-ring isomer **2a** had a twisted molecular structure and disjointed electronic configuration. On the other hand, the closed-ring isomer **2b** had a planar molecular structure and nondisjointed electronic configuration. The photoinduced change in magnetism agreed well with the expected change; the open-ring isomer has the "off" state and the closed-ring isomer has the "on" state.

(15) (a) Kobatake, S.; Yamada, T.; Uchida, K.; Kato, N.; Irie, M. *J. Am. Chem. Soc.* **1999**, *121*, 2380. (b) Kobatake, S.; Yamada, M.; Yamada, T.; Irie, M. *J. Am. Chem. Soc.* **1999**, *121*, 8450.

(16) Bleaney, B.; Bowers, K. D. *Proc. R. Soc. London* **1952**, *A214*, 451.

(17) The diamagnetic contribution was corrected by using Pascal's constants. The correction for the solvent in the crystal was also performed.

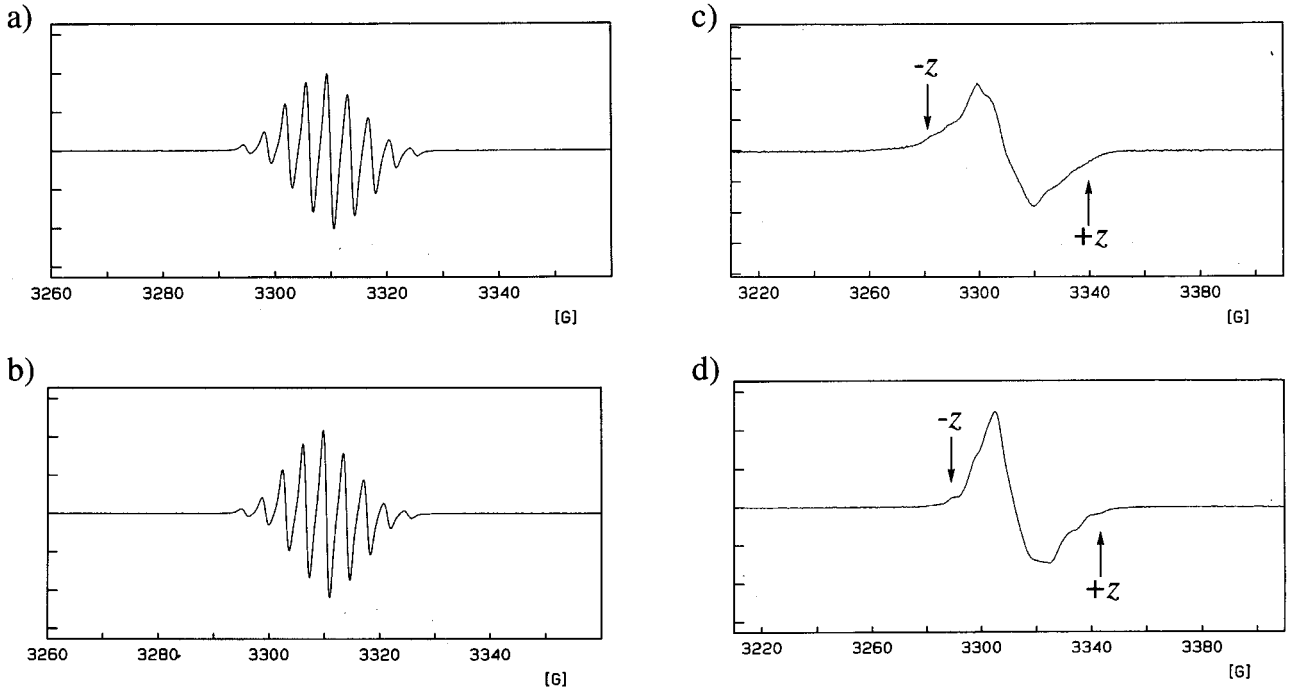

Figure 6. X-band ESR spectra of diradicals in solution at room temperature and in a glass matrix at cryogenic temperature. (a) **2a** (1.3 mM in benzene, room temperature, 9.32 GHz) and (b) **2b** (1.6 mM in benzene, room temperature, 9.32 GHz). For both **2a** and **2b**, hyperfine coupling constant $|a_N|$ and Landé g factor were determined as $|a_N| = 3.7$ G and $g = 2.006$. (c) **2a** (1 mM in MTHF, 8.0 K, 9.33 GHz) and (d) **2b** (1 mM in MTHF, 7.2 K, 9.33 GHz). For both **2a** and **2b**, zero-field splitting parameter $|D/hc| = 0.0026$ cm^{-1}.

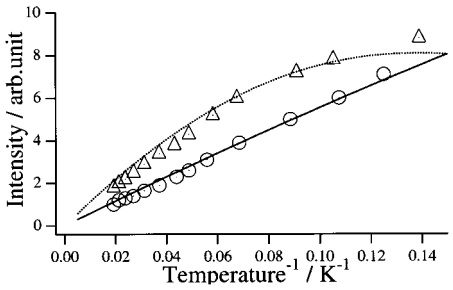

Figure 7. Intensities of the ESR signal at the $\Delta m_s = 1$ region for (○) **2a** and (△) **2b**. The solid and dotted lines indicate the theoretical curve of **2a** ($2J/k_B = -2.2$ K) and **2b** ($2J/k_B = -11.6$ K), respectively.

Switching of ESR Spectra. The ESR measurement was carried out for both **2a** and **2b** in benzene solution at room temperature and MTHF solid solution at cryogenic temperature (Figure 6). In solution at room temperature, both **2a** and **2b** showed nine lines centered at $g = 2.006$ with a hyperfine coupling constant $|a_N|$ of 3.7 G due to four equivalent nitrogen atoms, indicating that the exchange interactions between radicals were larger than the hyperfine coupling constant $|a_N|$. Since the hyperfine coupling constant is very small (the energy is equivalent to $\Delta E/k_B \approx 1 \times 10^{-3}$ K), there exist large interactions to give nine lines even in open-ring isomer **2a**.

ESR spectra of **2a** at 7.2 K and **2b** at 8.0 K showed broad lines with fine structures characteristic of triplet species in the $\Delta m_s = 1$ region for both open- and closed-ring isomers ($|D/hc| = 0.0026$ cm^{-1}). A half-field signal at the $\Delta m_s = 2$ region was not observed for either **2a** or **2b**. By point dipole approximation, the distance between radical centers was calculated to be 10 Å for both **2a** and **2b**. This distance agrees with the X-ray data. Since D values depend on dipole−dipole interaction between spins, not directly on exchange interaction, D values reflect directly spatial distance. No difference in the D values between **2a** and **2b** implies the distance between spins did not change by isomerization.

The temperature dependence of the signal intensity at $\Delta m_s = 1$ was measured and plotted as intensity vs reciprocal temperature (Curie plot, Figure 7). While the data of **2a** were straight because of the absence of strong interaction between spins, the data of **2b** were curved due to the notable exchange interaction. The data were consistent with the theoretical curve derived from the exchange interaction obtained from magnetic measurement. This result indicates that the intramolecular interaction was switched by photochromic spin coupler.

Switching of Electrochemical Properties. The electrochemical properties of diarylethenes **1a**, **1b**, **2a**, and **2b** was studied by means of cyclic voltammetry. The voltammograms are shown in Figure 8 and the numerical data are summarized in Table 4.

Table 4. Electrochemical Data for **1a**, **1b**, **2a**, and **2b** in Acetonitrile (V vs Ag/Ag$^+$)

diarylethene	diarylethene$^{\bullet -}$/ diarylethene E_{pc}	NN$^\bullet$/ NN$^+$ $E_{1/2}$	diarylethene/ diarylethene$^{\bullet +}$ E_{pa}
1a			
1b	−1.33		+1.05
2a		+0.46	
2b	−1.07	+0.52	+1.40

The orbital diagrams are also shown in Figure 9. While the open-ring isomer **1a** did not show any remarkable oxidation or reduction waves in the region from −2.2 to +1.6 V (vs Ag/Ag$^+$), the closed-ring isomer **1b** showed two quasi-reversible redox potentials at −1.33 and +1.05 V. The absorption wavelength calculated from the HOMO−LUMO gap was 520 nm, which is in good agreement with the value obtained by UV−visible absorption spectroscopy.[14]

2a had one reversible oxidation wave at +0.46 V due to the oxidation of nitronyl nitroxide. On the other hand, **2b** showed three redox potentials at −1.07, +0.52, +1.40 V. The oxidation

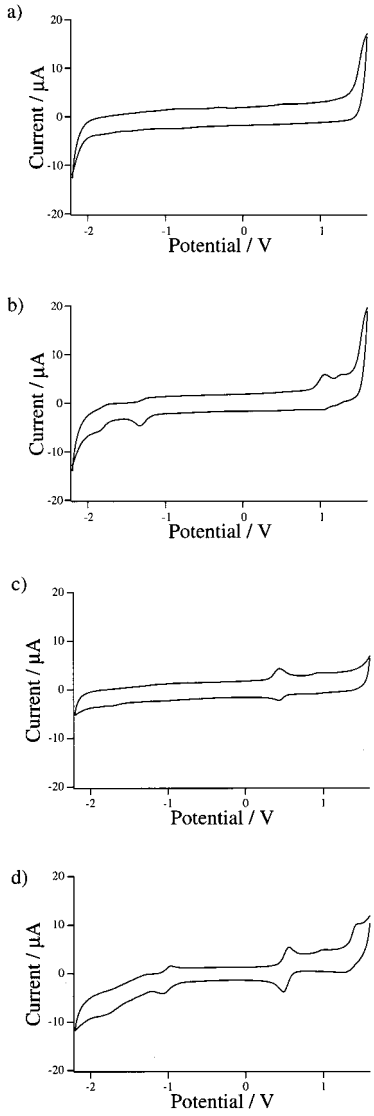

Figure 8. Cyclic voltammograms of(a) **1a**, (b) **1b**, (c) **2a**, and (d) **2b** in acetonitrile (0.1 M TBAP) on a platinum electrode (vs Ag/Ag^+). Scan rates were 200 mV/s.

potential of the diarylethene moiety of **2b** (+1.40 V) was 0.35 V more positive than that of **1b** (+1.05 V). This shift is attributable to the oxidation of the nitronyl nitroxide moiety of **2b** preceding the oxidation of the diarylethene moiety.

The oxidation at nitronyl nitroxide of **2b** occurred at almost the same potential as **2a** because the mixing of the SOMO of nitronyl nitroxide and HOMO of diarylethene was negligible because the SOMO of nitronyl nitroxide is localized at the ONCNO moiety of the radical.[18] The reduction potential of the diarylethene moiety of **2b** (−1.07 V) was 0.26 V less negative than that of **1b** (−1.33 V). This shift is attributable to the mixing of the LUMO of diarylethene with the LUMO of nitronyl nitroxide. The small shift of the oxidation potential of the nitronyl nitroxide between **2a** and **2b** indicates that the orbital interaction between nitronyl nitroxide and diarylethene is small. When the radicals of larger interaction with diarylethene are used, this shift should be larger.

Conclusions

We have developed a photochromic system, which reversibly changes the intramolecular magnetic interaction by photoirradiation. The change of magnetization was attributed to the change of the π-system. This is the first example of reversible switching of intramolecular magnetism. This is a potential photoswitch applicable to logic operation circuits.

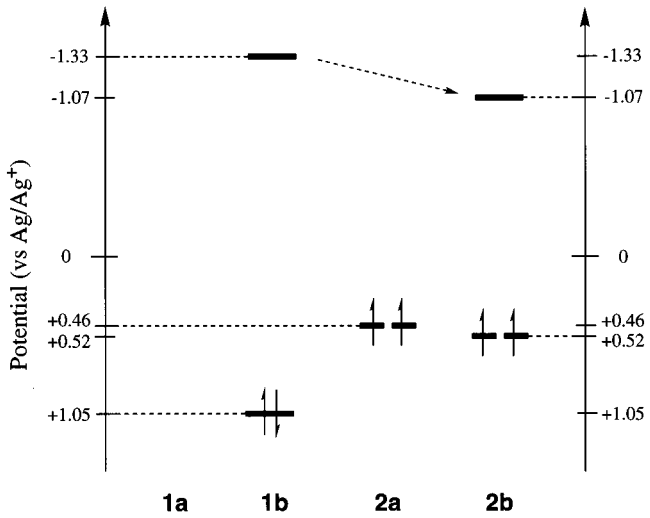

Figure 9. Potential diagram of **1a**, **1b**, **2a** and **2b**.

Experimental Section

A. Materials. ^{1}H NMR spectra were recorded on a Bruker AC-250P instrument. UV−visible spectra were recorded on a Hitachi U-3500 spectrophotometer. Mass spectra were obtained with JEOL JMS-HX110A instruments. Melting points are not corrected.

All reactions were performed under an atmosphere of dry argon unless otherwise specified. The reactions were monitored by thin-layer chromatography carried out on 0.2-mm E. Merck silica gel plates (60F-254). Column chromatography was performed on silica gel (E. Merck, 70−230 mesh).

1,2-Bis(6-formyl-2-methyl-1-benzothiophen-3-yl)hexafluorocyclopentene (4). To a stirred solution of 1,2-bis(2-methyl-1-benzothiophen-3-yl)hexafluorocyclopentene (**1a**; 2.35 g, 5.02 mmol) in nitrobenzene (25 mL) was added dichloromethyl methyl ether (7.5 mL) and anhydrous aluminum chloride (2.8 g) at 0 °C and stirred for 15 h at room temperature under argon atmosphere. Water was poured into the reaction mixture and then the product was extracted with ethyl acetate, washed with water, dried with magnesium sulfate, and concentrated. After evaporation of nitrobenzene in a vacuum, column chromatography (Hex:Et_2O = 3:1−1:1) gave diformyl compound **4** (2.16 g, 82%) as a white powder: mp 183.0−184.0 °C; ^{1}H NMR ($CDCl_3$, 250 MHz) δ 2.31 and 2.56 (s 2, 6 H), 7.68−8.20 (m, 6 H), 9.95 and 10.05 (s 2, 2 H). Anal. Calcd for $C_{25}H_{14}F_6O_2S_2$: C, 57.25; H, 2.69. Found: C, 57.22; H, 2.70.

1,2-Bis[6-(1-oxyl-3-oxide 4,4,5,5-tetramethylimidazolin-2-yl)-2-methyl-1-benzothiophen-3-yl]hexafluorocyclopentene (2a). A solution of **4** (2.0 g, 3.8 mmol), 2,3-bis(hydroxyamino)-2,3-dimethylbutane sulfate (4.75 g, 19.3 mmol), and potassium carbonate (2.85 g, 20.6 mmol) in methanol (40 mL) was refluxed for 24 h. The reaction mixture was poured into water, extracted with ethyl acetate, washed with water, dried over magnesium sulfate, and concentrated to give tetrahydroxylamine as yellow oil. Purification was not performed.

To a solution of tetrahydroxylamine in dichloromethane (300 mL) was added a solution of sodium periodate (2.45 g, 11.5 mmol) in water (500 mL), and the resultant mixture was stirred for 1 h in the open air. The organic layer was separated, washed with water, dried over magnesium sulfate, and concentrated. Purification was performed by column chromatography (silica, hexane:Et_2O = 1:1−0:1) followed by GPC and then the residue was recrystallized from CH_2Cl_2/hexane by the diffusion method in the dark. **2a** was obtained as dark blue microcrystalline (470 mg, 16%): mp 231.0−232.0 °C (dec); UV−vis (AcOEt) $\lambda_{max}(\epsilon)$ 300 (sh), 309 (3.4×10^4), 359 (sh), 377 (1.6×10^4), 553 (sh), 598 (6.3×10^2), 646 (6.3×10^2), 706 (sh); ESR (benzene)

(18) Kumai, R.; Matsushita, M. M.; Izuoka, A.; Sugawara, T. *J. Am. Chem. Soc.* **1994**, *116*, 4523.

1:4:10:16:19:16:10:4:1, 9 lines, $g = 2.007$, $|a_N| = 3.7$ G; FAB HRMS (m/z) $[M + H]^+$ calcd for $C_{37}H_{37}F_6N_4O_4S_2$, 779.2160; found, 779.2173.

Corresponding closed-ring isomer **2b**: black microcrystalline; UV−vis (AcOEt) $\lambda_{max}(\epsilon)$ 280 (1.7×10^4), 348 (1.9×10^4), 385 (sh), 400 (2.0×10^4), 565 (1.5×10^4); ESR (benzene) 1:4:10:16:19:16:10:4:1, 9 lines, $g = 2.007$, $|a_N| = 3.7$ G.

B. Photochemical Measurement. Absorption spectra were measured on a spectrophotometer (Hitachi U-3500). Photoirradiation was carried out by using a USHIO 500-W superhigh-pressure mercury lamp or a USHIO 500-W xenon lamp. Mercury lines of 313 and 578 nm were isolated by passing the light through a combination of Toshiba band-pass filter (UV-D33S) or sharp cut filter (Y-48, Y-52) and monochromator (Ritsu MC-20L).

C. Crystallography. The data collection was performed on a Bruker SMART1000 CCD-based diffractometer (50 kV, 40 mA) with Mo Kα radiation. The data were collected as a series of ω-scan frames, each with a width of 0.3°/frame. The crystal-to-detector distance was 5.118 cm. Crystal decay was monitored by repeating the 50 initial frames at the end data collection and analyzing the duplicate reflections. Data reduction was performed using SAINT software, which corrects for Lorentz and polarization effects and decay. The cell constants were calculated by the global refinement. The structure was solved by direct methods using SHELXS-86[19] and refined by full least-squares on F^2 using SHELXL-97.[20] The positions of all hydrogen atoms were calculated geometrically and refined by the riding model. The disordered part was refined isotropically.

D. ESR Spectroscopy. A Bruker ESP 300E spectrometer was used to obtain X-band ESR spectra. Temperatures were controlled by an RMC CT-470-ESR cryogenic temperature controller. The cryostat was maintained at high vacuum by a turbomolecular/rotary pump set. The sample was dissolved in solvent (∼1 mM) and degassed with argon bubbling for 5 min. The ESR intensities for Curie plots in the temperature range 7.2−50 K were measured at appropriate power attenuation calibrated to exclude saturation effect. The temperatures were stepped up from 7.2 to 50 K with intervals of ∼3 K.

E. Magnetic Measurement. A fine crystalline and polymer samples (>97.5% purity checked by HPLC) were mounted in a capsule and measured on a Quantum Design MPMS-5S SQUID susceptometer at 5000 G. Corrections for the diamagnetic contribution were made by using Pascal's constants.

F. Electrochemical Measurement. The measurement of electrochemical properties was performed on a BAS CV-50W electrochemical analyzer. Measurements were carried out in acetonitrile solution (∼1 mM) containing tetra(*n*-butyl)ammonium perchlorate (TBAP, 100 mM) as a supporting electrolyte. A three-electrode assembly (BAS) was used which was equipped with a platinum working electrode, a platinum coil as the counter electrode, and a Ag/Ag^+ (TBAP/acetonitrile) electrode as the reference electrode.

Acknowledgment. This work was supported by CREST of Japan Science and Technology Corp. and by a Grant-in Aid for Scientific Research on Priority Area "Creation of Delocalized Electronic Systems" (No. 12020244) from the Ministry of Education, Science, Culture, and Sports, Japan.

Supporting Information Available: X-ray structural information on **2a** and **2b** (PDF). An X-ray crystallographic file (CIF). This material is available free of charge via the Internet at http://pubs.acs.org.

JA000605V

(19) Sheldrick, G. M. *Acta Crystallogr., Sect. A* **1990**, *46*, 467−473.
(20) Sheldrick, G. M. *SHELXL-97*, Program for Crystal Structure Refinement; Universität Göttingen: Göttingen, 1997.